# Selected Overtone Mobility Spectrometry

Michael A. Ewing, Christopher R. P. Conant, Steven M. Zucker, Kent J. Griffith, and David E. Clemmer*

Department of Chemistry, Indiana University, Bloomington, Indiana 47405, United States

S *Supporting Information*

ABSTRACT: A new means of acquiring overtone mobility spectrometry (OMS) data sets that allows distributions of ions for a prescribed overtone number is described. In this approach, the drift fields applied to specific OMS drift regions are varied to make it possible to select different ions from a specific overtone that is resonant over a range of applied frequencies. This is accomplished by applying different fields for fixed ratios of time while scanning the applied frequency. The ability to eliminate peaks from all but a single overtone region overcomes a significant limitation associated with OMS analysis of unknowns, especially in mixtures. Specifically, *a priori* knowledge via selection of the overtone used to separate ions makes it possible to directly determine ion mobilities for unknown species and collision cross sections (assuming that the ion charge state is known). We refer to this selection method of operation as selected overtone mobility spectrometry (SOMS). A simple theoretical description of the SOMS approach is provided. Simulations are carried out and discussed in order to illustrate the advantages and disadvantages of SOMS compared with traditional OMS. Finally, the SOMS method (and its distinction from OMS) is demonstrated experimentally by examining a mixture of peptides generated by enzymatic digestion of the equine cytochrome *c* with trypsin.
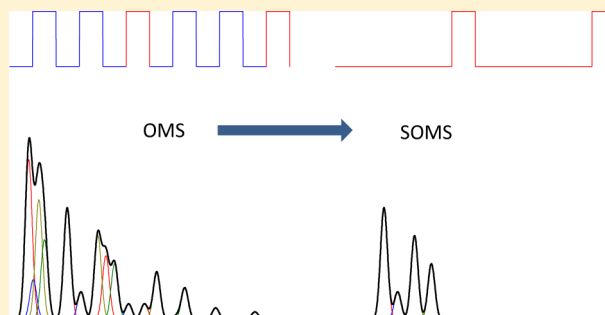
Advances in coupling linear drift tube ion mobility spectrometry (IMS) with mass spectrometry (MS)[1,2] are being applied to problems in emerging areas such as proteomics,[3,4] glycomics,[5,6] and structural biology.[7,8] This progress and the complexity of samples that are encountered in such applications have stimulated efforts to develop new mobility-based techniques, such as traveling wave ion mobility spectrometry,[9−11] whereby ions are advanced down the axis of a drift region using transient fields that resemble traveling waves; differential mobility analysis,[12−14] a long-standing technique, recently coupled to MS as a means of providing detailed information about macromolecular ions; field-asymmetric ion mobility spectrometry (sometimes called differential mobility spectrometry),[15−17] which separates ions based on differences in their low- and high-field mobilities; trapped IMS,[18,19] in which ions move against a gas flow when appropriate fields are applied; and transversal modulation ion mobility spectrometry,[20−22] in which the frequency of a transversal field orthogonal to the net ion motion determines whether ions exit an orifice or are neutralized on a plate, a technique which exhibits the same overtone problem as overtone mobility spectrometry (OMS). Recently, we have developed an approach called overtone mobility spectrometry.[23−30] OMS operates under the same conditions as linear drift tube IMS, separating ions by a mobility from which a collision cross section can be calculated, a parameter directly correlated to structure.[23,25] The resolving power of OMS scales nearly linearly with the length of the drift tube[24,25] (compared with the square root dependence upon length that is observed for IMS)[31] while also acting as a filter in a manner analogous to

a quadrupole mass spectrometer opening up potential analogous experiments with drift tubes. OMS uses alternating fields and a segmented drift tube with each segment containing a transmission region of length (l_t) and an elimination region of length (l_e). The elimination region is alternated between transmitting and eliminating states where ions can only pass through elimination regions during the transmitting state; ions traversing the elimination region during the eliminating state are neutralized, resulting in a selection of species with mobilities that are resonant with the frequency of a set of applied alternating fields. An outcome of scanning the frequency (f) of the applied fields is that ions can be transmitted at certain multiples (each characterized by its OMS frequency coefficient, m) of the fundamental resonance frequency (f_f). Ions of a given mobility, K, are selected when $1/f$ or m/f corresponds to the time it takes to traverse a single segment as given in eq 1,

$$K = \frac{f(l_t + l_e)}{mE}$$

(1)

where E is the magnitude of the applied electric field. By scanning the frequency, a family of peaks are generated for a single ion. The method of ion selection and transmission and of spectrum acquisition in OMS has been described in more detail previously.[24−26,30]

One limitation of OMS is that the frequencies used to transmit the same ions at different values of m may overlap.

This is especially problematic when working in high-overtone regions, which is desirable because of increases in resolving power that occur with increasing m.[24,25] The inability to unambiguously assign an overtone to specific peaks in regions where they may overlap complicates the interpretation of data, especially when analyzing complex mixtures.[27] Because m is not known *a priori*,[23,25,27] it is not possible to determine the mobility directly for any peak in the spectrum. Without such information, one cannot determine reduced mobilities or collision cross sections directly from overlapping regions of the OMS spectrum.

In this paper, we describe a technique for selecting specific overtones within the OMS spectrum, selected overtone mobility spectrometry (SOMS), that we recently proposed.[29] SOMS operates by changing the length of time for which different phases are applied to selectively transmit only certain packets from a train of OMS packets. By applying phases for unequal lengths of time, some overtones are selected while others are not as described in detail below. The approach dramatically simplifies spectra in regions where peaks may overlap, facilitating the analysis of complex mixtures of ions and, as noted, the definition of m makes it possible to directly determine mobilities. Below, we provide a simple theoretical description of the selection process as well as simulations and experiments demonstrating the approach. This ability to define the overtone frequency coefficient from instrument parameters provides direct measurement of the mobility as well as several other advantages that are also discussed.

■ THEORETICAL

OMS Background. In order to understand SOMS, it is useful to begin with a brief theoretical overview of OMS. As described in detail previously,[25,26] in OMS, sets of drift voltages are applied (at defined values of f) to multiple drift regions in a sawtooth pattern to generate different fields in different regions of the instrument. The number of different applied electric fields is defined as the phase, ϕ, which also defines the number of segments before the applied voltages repeat within an OMS instrument. Here, we present the case for $\phi = 2$, for which there are two applied fields and either a given elimination region is active or its nearest neighbor elimination regions are active. An elimination region is active in OMS when the applied fields direct ions toward a conductive surface in order to neutralize or eliminate them, and it is inactive when the potentials applied direct ions to pass through to the next stage of the instrument (typically another segment). When f is scanned, the preferential elimination of ions with unmatched mobilities yields OMS peaks across the range of applied drift field frequencies; ignoring diffusion, the resolving power of this method scales linearly with length and with overtone coefficient.[24,25] This is in contrast to traditional IMS where the resolving power scales with the square root of the length of the drift region.[31] While scaling with length in IMS is due to diffusional effects, diffusional effects are significantly less important to OMS resolving power. A full treatment of the comparison of scaling of the resolving powers is outside the scope of this manuscript but has been described in detail previously.[25]

Despite the increased resolving power, the peak capacity of OMS is limited by the overlap of overtones,[27] which increases with m. Peaks overlap when ions having different mobilities traverse the drift tube at overlapping frequencies in a manner that can be described using the segment traversal time (t_{seg}), the average time it takes an ion to traverse a single segment. If there is overlap, the ratio between the two segment traversal times $t_{seg,1}/t_{seg,2} \approx m_1/m_2$, such that m_1 and m_2 are both OMS frequency coefficients allowed by a given geometry and phase pattern as described previously.[25,26] Selection of overtones can thus be achieved by reducing the number of permitted OMS frequency coefficients.

In developing an understanding of OMS, one sees also that the physical length of the stable transmitting ion packet is directly proportional to the range of times for which ions from a given packet traverse a given elimination region.[28] As described in previous work,[28] the length of the transmitting ion packet is a key factor in defining three major characteristics of overtone peaks: OMS frequency coefficient, resolving power, and transmission efficiency.[28] To select specified overtones, we introduce a method of pulsing the fields that yields the same timing of packets of OMS of the same m and yields the same transmitting packet length.

Figure 1 shows an illustration of ion packets progressing in time for transmission of a single ion type at values of $m = 1$, 3, and 5 through a hypothetical OMS device comprised of six drift tube segments. For purposes of simplicity, we have not included diffusion. In this illustration, ions enter the instrument from the left and exit on the right. For the first snapshot of each
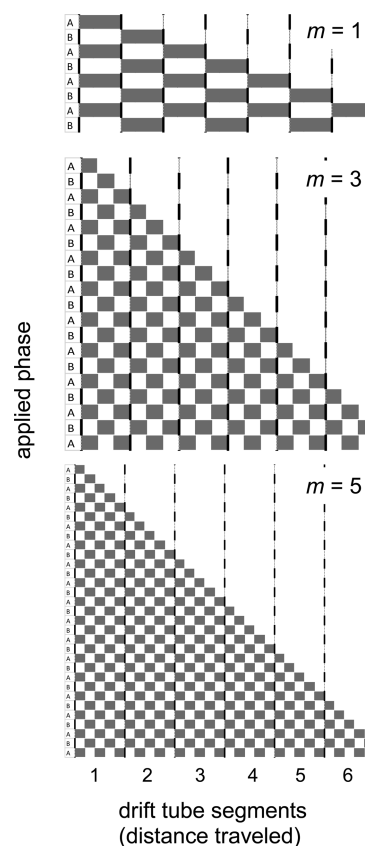

Figure 1. Schematics of ion packet motion for OMS at frequencies corresponding to $m = 1$, 3, and 5. At f_b, ions travel one segment during the length of time of each applied phase, and therefore at $f = mf_b$, ions travel $1/m$ of the length of a segment for each applied phase. Along the left side, each snapshot shows the position of the packet at the end of an application of the phase shown on the left, each phase being applied for a length of time of $1/f$. Vertical bold lines indicate active elimination regions whereas dashed vertical lines indicate inactive elimination regions. Each schematic progresses in time to show the first repeat of a previous step.

illustration (top left), ions are stable if they enter the instrument when the phase A sawtooth is applied and unstable when phase B is applied. After the appropriate delay period, the waveform is switched to the phase B sawtooth such that ions can no longer enter the device. When the phase A waveform is reapplied, a new packet of ions enters. In this way, the device is filled with 50% of the ions and 50% of the ions are eliminated. The primary difference between the $m = 1$, 3, and 5 conditions is the length and number of stable ion packets. We have previously shown illustrations and simulations of how scanning the drift field frequency leads to the OMS spectrum.[24,25]

Selection of Specified Overtones. As mentioned in the introduction, application of different phases for different periods of time are employed to manipulate which packet lengths (and, thus, which overtones) progress down the drift tube. Consider a case where phase B is applied for a factor of 5 times as long as phase A. Figure 2 shows an illustration of how
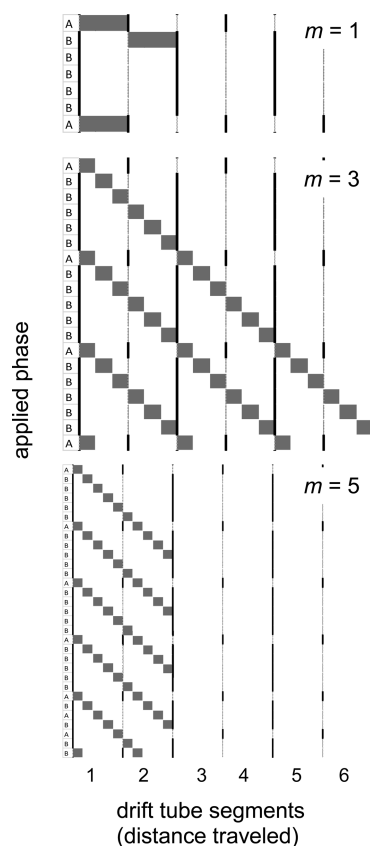
Figure 2. Schematics of ion packet motion for SOMS with $\zeta_B = 5$ at frequencies corresponding to $m = 1$, 3, and 5. The schematic is otherwise organized in the same manner as Figure 1. Ions transmit through the six segments only at the frequency corresponding to $m = 3$ whereas at frequencies corresponding to $m = 1$ and 5 the ions do not transmit through the instrument.

packets of ions will be transmitted through the same hypothetical device as was discussed in Figure 1 for OMS. In this case, only the frequency corresponding to $m = 3$ is transmitted through the entire instrument. This is the conceptual framework for SOMS.

It is worthwhile to formalize these ideas. For the simplest two-phase system, we can define a phase ratio, ζ_B, as the ratio of time in a single (equivalent or longer) phase B to the time in a single (equivalent or shorter) phase A. With this, we define f_{soms}

to be the inverse of the shortest drift field application time (for OMS, f is the inverse of the drift field application time). Thus, a scan of frequency is a scan of one variable and determines the drift field application time both for phase A and for phase B. With this, eq 2 describes the SOMS frequency coefficient, μ, a geometry-independent, phase-application-dependent parameter that is similar to m;

$$\mu = \frac{\zeta_B + 1}{2} \tag{2}$$

From Figures 1 and 2, we observe that μ corresponds to a selected m. That is, overtone peaks with $m < \mu$ are not observed for SOMS of a given μ and even overtones above $m > \mu$ are often not observed, although we will note their appearance empirically below at frequencies of $m\mu f_f$. SOMS operates by selecting every μth packet. In Figure 2, is it clear that, by spending unequal amounts of time in different phases, the packet corresponding to the fundamental frequency (defined by a packet length equal to a transmission region as described previously[28]) is unable to transmit the instrument. Similarly, it is obvious that the ratio of time spent in each phase can prohibit higher overtones as well. Intriguingly, eq 2 indicates that it is possible to transmit ions using noninteger overtone coefficients even with two-phase SOMS.

■ EXPERIMENTAL SECTION

Simulations. Simulations were carried out using software written in-house for simulation of ion motion, as described previously.[23,25,26,32] Briefly, SIMION 8.0[33] was used for the generation of electric fields. Ions were then moved on the basis of the sum of electric field directed motion and Brownian motion, modeled as a Gaussian function.[31] A drift tube modeled after the original OMS drift tubes[24] was constructed in SIMION with a transmission length of 5.38 cm and an elimination length of 0.50 cm, 24 segments, and an electric field of 8 V·cm^{-1}. For these simulations, we chose mobilities corresponding to doubly protonated substance P (having a reduced mobility, $K_0 = 3.41$ cm^{2}V^{-1}s^{-1})[34] and singly protonated polyalanine (A_n, where $n = 3$ to 19, and respective K_0s, reported elsewhere[35]).

Specific Conditions for Substance P. In the frequency regions for OMS frequency coefficients of 1, 3, and 5, simulations were performed with 10^5 ions at 10^3 evenly spaced unique positions across the first two segments (10^6 ions were used for the 7 and 9 coefficients). For OMS and SOMS simulations of the overtone coefficients of 1, 3, and 5, field application time (the length of time for which a single phase is applied, $1/f$) was scanned (in μs) from 370.0 to 570.0, from 150.0 to 161.0, and from 92.6 to 95.8 in increments of 0.2. For regions of the spectra not expected to have any peaks, the field application time was scanned from 96.0 to 150.0, 161.0 to 370.0, and 570.0 to 1000.0, in increments of 1.0. Time steps of 0.1 μs were used for all these simulations. The entire range from 51.0 to 1000.0 was scanned for all simulations. For the overtone coefficients of 7 and 9, field application time was scanned (in μs) from 65.8 to 68.0 and from 51.0 to 53.0 in increments of 0.1. To ensure that no extra peaks in unexpected regions of the spectra were present, the field application time was also scanned from 53.0 to 65.8 and 68.0 to 92.6, in increments of 0.5. Time steps of 0.01 μs were used for these simulations.

As alluded to in eq 2, it is also possible to transmit selected noninteger overtone coefficient regions. We illustrate this using

an overtone coefficient of 1.125; field application time was scanned (in μs) from 13.0 to 59.9 in increments of 0.1, 60.0 to 78.4 in increments of 0.2, 79.0 to 132.0 in increments of 0.5, and 132.0 to 395.0 in increments of 1.0. To simulate SOMS equivalent to an overtone of 1.125, the above field application times were applied to a set of four consecutive applied phase As followed by five consecutive phase Bs. Time steps for these simulations were all 0.1 μs.

Specific Conditions for Polyalanine. Simulations for each of the 17 different polyalanine ions were initiated using 10^4 ions across 10^3 unique positions and a time step of 0.01 μs. The field application time (in μs) was scanned from 25.00 to 50.00 in increments of 0.05, 50.0 to 86.0 in increments of 0.1, 86.0 to 110.0 in increments of 0.2, 110.0 to 155.0 in increments of 0.5, 155.0 to 250.0 in increments of 1.0, and 250 to 900 in increments of 5. All OMS simulations were performed by repeating a sequence consisting of one phase A and one phase B while all SOMS simulations were performed by repeating a sequence consisting of one phase A followed by 5 consecutive applications of phase B, each for the same length of time as the phase A.

Instrumentation and Measurements. A gridless OMS instrument described previously[30] was used to analyze samples and demonstrate selection of overtones. Briefly, experiments were carried out as follows. A mixture of tryptic peptides from equine cytochrome c (Sigma-Aldrich [St. Louis, MO]) was dissolved in 49/49/2 water/acetonitrile/acetic acid solution at a concentration of ~0.1 mg/mL and continuously electrosprayed into a home-built ion source as described previously.[36] The continuous ion beam is introduced into a gridless OMS instrument, which has been described previously.[30] Those ions that exit the OMS device are introduced into a home-built reflectron time-of-flight MS instrument where they are mass-analyzed and detected. The OMS instrument is operated at a pressure of 2.69 Torr and a temperature of 300 K; all other aspects of the gridless OMS instrument are identical to those described previously[30] with the exception of the applied drift field phases necessary for SOMS.

Acquisition of OMS and SOMS Data Sets. A home-built field programmable gate array-based pulser with 8 ns resolution was used to generate pulse sequences corresponding to desired lengths of time in phases for conventional OMS and desired SOMS. These pulses were then used to set the output phase from a home-built wavedriver[37] that applied voltages in a sawtooth pattern to the OMS lenses for each of two phases. Each mass spectrum was collected for 10 s, and the field application frequency was scanned from 1000 to 28 000 Hz in increments of 50 Hz.

■ RESULTS AND DISCUSSION

SOMS Simulations of Substance P. While Figures 1 and 2 demonstrate that selection of overtones should be possible, simulations are valuable in understanding SOMS in more detail. Figure 3 shows a comparison of OMS and SOMS simulations for substance P. The outcome of the SOMS simulation with a phase ratio of $\zeta_B = 5$ (and SOMS frequency coefficient $\mu = 3$) shows that a single peak at a frequency of 6418 Hz is observed. As expected from the theoretical conditions, this corresponds to the selection of the $m = 3$ peak for substance P that is observed in the OMS simulation. Inspection of these simulations shows that the resolving power that is obtained for the OMS $m = 3$ and SOMS-simulated peaks is equivalent. Also shown in Figure 3 is a SOMS spectrum generated for the
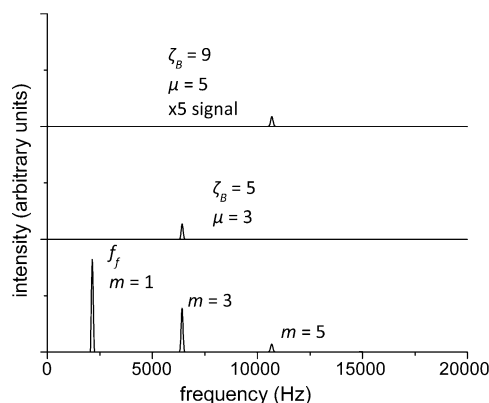

Figure 3. Simulated spectra for substance P for OMS (all overtones, bottom spectrum), SOMS with $\zeta_B = 5$ and $\mu = 3$ (middle spectrum), and SOMS with $\zeta_B = 9$ and $\mu = 5$ (top spectrum). As indicated in the figure, the signal at $\mu = 3$ is 1/3 the signal at $m = 3$ in the OMS spectrum and the signal at $\mu = 5$ is 1/5 the signal at $m = 5$ in the OMS spectrum.

condition of $\zeta_B = 9$ ($\mu = 5$). As expected, these conditions lead to a selection of the $m = 5$ region of the OMS spectrum, and the resolving power associated with the SOMS simulation is equivalent to that of the OMS simulation in the $m = 5$ region.

One difference that is observed between equivalent regions of the OMS and SOMS simulations is associated with the intensities of peaks. The simulations for SOMS show that fewer ions are transmitted upon selection, compared with the equivalent OMS region. This decrease in transmission of SOMS (reduction in signal by a factor of μ) is consistent with the predictions from theory and can be observed (without inclusion of diffusion) in Figures 1 and 2. In a previous gridless OMS instrument, we have reported detecting 20 attomoles of angiotensin I with a signal/noise of ~5 at the third overtone when the gridless OMS device was incorporated into a larger home-built IMS-TOF-MS device.[30]

As mentioned above, eq 2 suggests that noninteger selections are accessible with some two-phase SOMS conditions. This outcome was not immediately intuitive to us, as it effectively raises the possibility of using SOMS to work in regions where the OMS distribution is forbidden. For example, in two-phase OMS, the second overtone ($m = 2$) region is never transmitted or observed using OMS (in simulations or real experiments).[25,26] However, from eq 2, we see that application of SOMS using $\zeta_B = 3$ [i.e., where $\mu = (3 + 1)/2 = 2$] leads to selection of a frequency region that corresponds to the hypothetical $m = 2$ region of OMS: a region that for OMS is *forbidden*! Thus, it is interesting to simulate these regions to see if ions are transmitted.

Figure 4 shows two examples of simulations of SOMS conditions that lead to selection of *forbidden* OMS regions. The first is the $\zeta_B = 3$ condition, that effectively selects what would be the $m = 2$ region of OMS; the second is a noninteger region, which we have chosen using $\zeta_B = 1.25$, effectively the $m = 1.125$ forbidden region of OMS, which we define using the new SOMS frequency coefficient, $\mu = 1.125$. Clearly, from these arguments, we have not really selected something that is forbidden; rather, the new experimental conditions make it possible to choose any frequency range in which to evaluate ions. Once this new SOMS frequency range is selected for any ions, we observe a new set of additional peaks for the selected peak. Figure 4 shows these additional peaks at $m\mu = 6$ (i.e., 3·2)
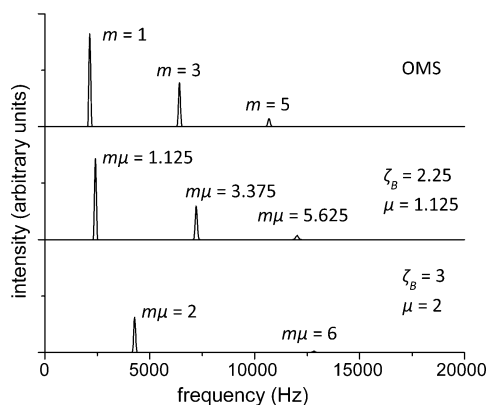
Figure 4. Simulated spectra for substance P for OMS (all overtones, top spectrum), SOMS with $\zeta_B = 3$ and $\mu = 2$ (bottom spectrum), and SOMS with $\zeta_B = 1.25$ and $\mu = 1.125$ (middle spectrum). As described in the text, SOMS selected overtones need not be overtones observed in OMS. Additionally, a new series of low-insensity $m\mu$ overtones is observed with SOMS. Resolving powers are shown in Table S-1, Supporting Information. See text for details.

from $\zeta_B = 3$, as well as $m\mu$ values of 3.375 (i.e., 3·1.125) and 5.625 (i.e., 5·1.125) from $\zeta_B = 1.25$.

While these peaks are effectively new overtone bands associated with the new selected regions, the SOMS approach allows us to control the position of these features such that it is possible to minimize overlap of multiple regions of the spectrum. Additionally, the ability to position the frequency ranges that are used in these analyses has direct advantages associated with resolving power and peak capacity (as discussed previously),[27,28] but it is important to note that, at the $\zeta_B = 1$ extreme, SOMS is equivalent to OMS. This is not true at higher ζ_B values; that is, it is feasible to select a series of overtones such that only one selected overtone is observed with the rest being above the maximum overtone that can be transmitted.[28]

SOMS Simulations of a Mixture of Polyalanine Species. To understand how SOMS could be applied to enable analyses of complex mixtures, we simulated a range of 17 singly protonated polyalanine species (Ala$_3$, Ala$_4$, Ala$_5$, ..., Ala$_{19}$, respectively). Figure 5 shows the resulting simulated
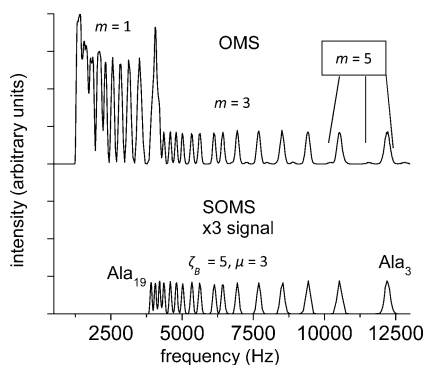

Figure 5. Simulated spectra for OMS (top) and SOMS (bottom) with $\zeta_B = 5$ for equal ion intensities of polyalanine ranging from 3 to 19 residues. The SOMS spectrum exhibits 17 peaks, one for each component and all corresponding to the $m = 3$ overtone, whereas the peaks in the OMS spectrum from different overtones overlap, complicating identification of each peak. Resolving powers for the $m = 3$ and corresponding selected peaks are shown in Table S-2, Supporting Information.

OMS and SOMS spectra ($\mu = 3$), respectively. Because of the equal abundances of each ion at the start of the simulation, it is possible (although not easy) to discern which peaks are associated with $m = 1$, 3, and 5; the $m = 1$ peaks are much larger than the $m = 3$ peaks which are much larger than the barely visible $m = 5$ peaks. Despite this difference in intensity, the overlap in frequencies between the regions associated with each overtone leads to an inability to distinguish all of the species in OMS, and it would not be possible to determine values of K_0 for peaks similar to these from measurements. The SOMS spectrum, on the other hand, distinguishes all 17 species quite cleanly, enabling a straightforward assignment of each of the species in the mixture. Because the m value is selected, it would be possible to directly determine K_0 values from experimental measurements of this kind.

SOMS Demonstration Using Tryptic Peptides from Cytochrome c. As a final illustration of SOMS, we have examined a mixture of peptides using a new gridless OMS instrument.[30] The maximum overtone for this instrument is slightly greater than 5,[30] yielding the fundamental frequency and overtones corresponding to $m = 3$ and $m = 5$, with signal from $m = 5$ peaks being lower compared to the other peaks. Figure 6 shows OMS-MS and SOMS-MS plots of a tryptic digest of cytochrome c. At low frequencies, we transmit species in the f_f region of the distribution. The same distribution of ions is observed at the $m = 3$ and 5 higher overtone regions (although at higher resolving power and lower intensities as discussed previously[24,25,30]). We have highlighted the multiple observation of ions by annotating the position of the
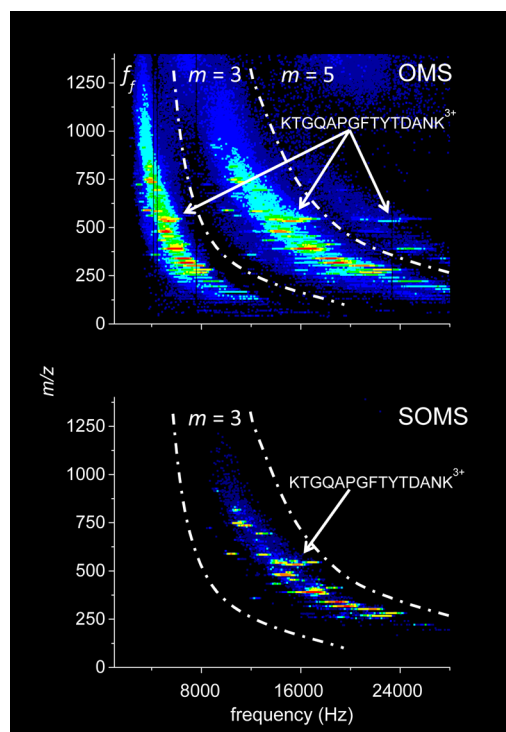

Figure 6. Two-dimensional OMS-MS (top) and SOMS-MS (bottom) spectra, where blue represents least intense peaks and red represents most intense peaks corresponding to tryptic peptide ions generated upon electrospraying a tryptic digest of cytochrome c. A SOMS selection of the $\mu = 3$ overtone region was employed to produce the bottom spectrum which selects the $m = 3$ peaks of OMS. See text for details.

$[KTGQAPGFTYTDANK + 3H]^{3+}$ ion in different regions of the OMS spectrum. As discussed, analysis of the complex mixture of ions with OMS shows that transmission regions overlap in frequency. Thus, without prior knowledge, we could not derive values of K_0 directly from these OMS data without making an assumption as to the value of m. Moreover, the center of the SOMS ($\mu = 3$) peak corresponds to a value of K_0 ($[KTGQAPGFTYTDANK + 3H]^{3+}$) = 5.22 cm^{2}V^{-1}s^{-1}; this value is identical within experimental uncertainties (~±1% relative error) to the value of K_0 = 5.25 cm^{2}V^{-1}s^{-1} obtained in a prior measurement.[36] The resolving power for this measurement is ~15 to 20 for many peaks. Finally, as predicted from theory and simulations, the experimental spectrum is greatly simplified.

■ CONCLUSION

We presented theory, simulations, and experiments showing that SOMS enables specific overtone regions of an OMS distribution to be selected. This new method appears to have significant utility in advancing mobility-based separations. We cannot resist noting that these types of mobility-based filters are analogous in some ways to quadrupole mass filters; thus, although SOMS devices are at a very early stage, we envision quadrupole-like SOMS applications, although selection would be based on uniqueness of mobility rather than mass.

■ ASSOCIATED CONTENT

Ⓢ Supporting Information

The resolving powers of $m = 3$ peaks from OMS mode simulations and corresponding peaks from SOMS mode simulations in Figures 4 and 5. The Supporting Information is available free of charge on the ACS Publications website at DOI: 10.1021/ac504555u.

■ AUTHOR INFORMATION

Corresponding Author

*E-mail: clemmer@indiana.edu.

Notes

The authors declare the following competing financial interest(s): The authors declare a submitted patent associated with this idea: US Patent App. 13/844,901, 2013.

■ ACKNOWLEDGMENTS

■ REFERENCES

(1) Hoaglund, C. S.; Valentine, S. J.; Sporleder, C. R.; Reilly, J. P.; Clemmer, D. E. *Anal. Chem.* **1998**, *70*, 2236−2242.

(2) Henderson, S. C.; Valentine, S. J.; Counterman, A. E.; Clemmer, D. E. *Anal. Chem.* **1999**, *71*, 291−301.

(3) Baker, E. S.; Burnum-Johnson, K. E.; Jacobs, J. M.; Diamond, D. L.; Brown, R. N.; Ibrahim, Y. M.; Orton, D. J.; Piehowski, P. D.; Purdy, D. E.; Moore, R. J.; Danielson, W. F.; Monroe, M. E.; Crowell, K. L.; Slysz, G. W.; Gritsenko, M. A.; Sandoval, J. D.; LaMarche, B. L.; Matzke, M. M.; Webb-Robertson, B. J. M.; Simons, B. C.; McMahon, B. J.; Bhattacharya, R.; Perkins, J. D.; Carithers, R. L.; Strom, S.; Self, S. G.; Katze, M. G.; Anderson, G. A.; Smith, R. D. *Mol. Cell Proteomics* **2014**, *13*, 1119−1127.

(4) McLean, J. A.; Ruotolo, B. T.; Gillig, K. J.; Russell, D. H. *Int. J. Mass Spectrom.* **2005**, *240*, 301−315.

(5) Li, H. L.; Bendiak, B.; Kaplan, K.; Davis, E.; Siems, W. F.; Hill, H. H. *Int. J. Mass Spectrom.* **2013**, *352*, 9−18.

(6) Williams, J. P.; Grabenauer, M.; Holland, R. J.; Carpenter, C. J.; Wormald, M. R.; Giles, K.; Harvey, D. J.; Bateman, R. H.; Scrivens, J. H.; Bowers, M. T. *Int. J. Mass Spectrom.* **2010**, *298*, 119−127.

(7) Bernstein, S. L.; Duipuis, N. F.; Lazo, N. D.; Wyttenbach, T.; Condron, M. M.; Bitan, G.; Teplow, D. B.; Shea, J. E.; Ruotolo, B. T.; Robinson, C. V.; Bowers, M. T. *Nat. Chem.* **2009**, *1*, 326−331.

(8) Uetrecht, C.; Barbu, I. M.; Shoemaker, G. K.; van Duijn, E.; Heck, A. J. R. *Nat. Chem.* **2011**, *3*, 126−132.

(9) Giles, K.; Pringle, S. D.; Worthington, K. R.; Little, D.; Wildgoose, J. L.; Bateman, R. H. *Rapid Commun. Mass Spectrom.* **2004**, *18*, 2401−2414.

(10) Pringle, S. D.; Giles, K.; Wildgoose, J. L.; Williams, J. P.; Slade, S. E.; Thalassinos, K.; Bateman, R. H.; Bowers, M. T.; Scrivens, J. H. *Int. J. Mass Spectrom.* **2007**, *261*, 1−12.

(11) Giles, K.; Williams, J. P.; Campuzano, I. *Rapid Commun. Mass Spectrom.* **2011**, *25*, 1559−1566.

(12) Rosell-Llompart, J.; Loscertales, J. G.; Bingham, D.; Fernandez de la Mora, J. *J. Aerosol Sci.* **1996**, *27*, 695−719.

(13) Kaufman, S. L.; Skogen, J. W.; Dorman, F. D.; Zarrin, F.; Lewis, K. C. *Anal. Chem.* **1996**, *68*, 1895−1904.

(14) Rus, J.; Moro, D.; Sillero, J. A.; Royuela, J.; Casado, A.; Estevez-Molinero, F.; de la Mora, J. F. *Int. J. Mass Spectrom.* **2010**, *298*, 30−40.

(15) Gorshkov, M. P. U.S.S.R. Inventor's Certificate 966583, 1982.

(16) Purves, R. W.; Guevremont, R.; Day, S.; Pipich, C. W.; Matyjaszczyk, M. S. *Rev. Sci. Instrum.* **1998**, *69*, 4094−4105.

(17) Shvartsburg, A. A.; Seim, T. A.; Danielson, W. F.; Norheim, R.; Moore, R. J.; Anderson, G. A.; Smith, R. D. *J. Am. Soc. Mass Spectrom.* **2013**, *24*, 109−114.

(18) Fernandez-Lima, F.; Kaplan, D. A.; Suetering, J.; Park, M. A. *Int. J. Ion Mobility Spectrom.* **2011**, *14*, 93−98.

(19) Silveira, J. A.; Ridgeway, M. E.; Park, M. A. *Anal. Chem.* **2014**, *86*, 5624−5627.

(20) Vidal-de-Miguel, G.; Macia, M.; Cuevas, J. *Anal. Chem.* **2012**, *84*, 7831−7837.

(21) Vidal-de-Miguel, G.; Macia, M.; Barrios, C.; Cuevas, J. *Anal. Chem.* **2015**, *87*, 1925−1932.

(22) Barrios-Collado, C.; Vidal-de-Miguel, G. *Int. J. Mass Spectrom.* **2015**, *376*, 97−105.

(23) Lee, S.; Ewing, M. A.; Nachtigall, F. M.; Kurulugama, R. T.; Valentine, S. J.; Clemmer, D. E. *J. Phys. Chem. B* **2010**, *114*, 12406−12415.

(24) Kurulugama, R.; Nachtigall, F. M.; Lee, S.; Valentine, S. J.; Clemmer, D. E. *J. Am. Soc. Mass Spectrom.* **2009**, *20*, 729−737.

(25) Valentine, S. J.; Stokes, S. T.; Kurulugama, R.; Nachtigall, F. M.; Clemmer, D. E. *J. Am. Soc. Mass Spectrom.* **2009**, *20*, 738−750.

(26) Valentine, S. J.; Kurulugama, R. T.; Clemmer, D. E. *J. Am. Soc. Mass. Spectrom.* **2011**, *22*, 804−16.

(27) Kurulugama, R. T.; Nachtigall, F. M.; Valentine, S. J.; Clemmer, D. E. *J. Am. Soc. Mass Spectrom.* **2011**, *22*, 2049−2060.

(28) Ewing, M. A.; Zucker, S. M.; Valentine, S. J.; Clemmer, D. E. *J. Am. Soc. Mass Spectrom.* **2013**, *24*, 615−621.

(29) Clemmer, D. E.; Ewing, M. A.; Zucker, S. M.; Conant, C. R. P. *Ion mobility spectrometer and method of operating same.* US Patent App. 13/844,901, 2013.

(30) Zucker, S. M.; Ewing, M. A.; Clemmer, D. E. *Anal. Chem.* **2013**, *85*, 10174−10179.

(31) Mason, E. A.; McDaniel, E. W. *Transport Properties of Ions in Gases*; Wiley: New York, 1988; pp 1−27, 137−223.

(32) Koeniger, S. L.; Merenbloom, S. I.; Valentine, S. J.; Jarrold, M. F.; Udseth, H.; Smith, R.; Clemmer, D. E. *Anal. Chem.* **2006**, *78*, 4161−4174.

(33) *SIMION ver. 8.0*; Scientific Instrument Services Inc.: Ringoes, NJ, USA, 2006.

(34) Myung, S.; Lee, Y. J.; Moon, M. H.; Taraszka, J.; Sowell, R.; Koeniger, S.; Hilderbrand, A. E.; Valentine, S. J.; Cherbas, L.; Cherbas, P.; Kaufmann, T. C.; Miller, D. F.; Mechref, Y.; Novotny, M. V.; Ewing, M. A.; Sporleder, C. R.; Clemmer, D. E. *Anal. Chem.* **2003**, *75*, 5137−5145.

(35) Henderson, S. C.; Li, J.; Counterman, A. E.; Clemmer, D. E. *J. Phys. Chem. B* **1999**, *103*, 8780−8785.

(36) Dilger, J. M.; Valentine, S. J.; Glover, M. S.; Ewing, M. A.; Clemmer, D. E. *Int. J. Mass Spectrom.* **2012**, *330−332*, 35−45.

(37) Merenbloom, S. I.; Glaskin, R. S.; Henson, Z. B.; Clemmer, D. E. *Anal. Chem.* **2009**, *81*, 1482−1487.